Neuro-Oncology Advances
3(1), 1–13, 2021 | https://doi.org/10.1093/noajnl/vdab104 | Advance Access date 18 August 2021

Intracranially injectable multi-siRNA nanomedicine for the inhibition of glioma stem cells

Cheripelil Abraham Manju, Kottarapat Jeena, Ranjith Ramachandran, Maneesh Manohar, Anna Mathew Ambily, Koythatta Meethalveedu Sajesh, Genekehal Siddaramana Gowd, Krishnakumar Menon, Keechilat Pavithran, Ashok Pillai, Shantikumar V. Nair, and Manzoor Koyakutty

Centre for Nanosciences and Molecular Medicine, Amrita Vishwa Vidyapeetham, Kochi, Kerala, India (C.A.M., K.J., R.R., M.M., A.M.A., K.M.S., D.C., G.S.G., K.K.M., S.V.N., M.K.); Department of Neurosurgery, Amrita Institute of Medical Sciences, Amrita Vishwa Vidyapeetham, Kochi, Kerala, India (A.P.); Department of Oncology, Amrita Institute of Medical Sciences, Amrita Vishwa Vidyapeetham, Kochi, Kerala, India (K.P.)

Corresponding Author: Manzoor Koyakutty, PhD, Centre for Nanosciences and Molecular Medicine, Amrita Vishwa Vidyapeetham, Kochi 682 041, Kerala, India (manzoork@aims.amrita.edu).

Abstract

Background. Nanoparticle siRNA-conjugates are promising clinical therapeutics as indicated by recent US-FDA approval. In glioma stem cells (GSC), multiple stemness associated genes were found aberrant. We report intracranially injectable, multi-gene-targeted siRNA nanoparticle gel (NPG) for the combinatorial silencing of 3 aberrant genes, thus inhibiting the tumorogenic potential of GSCs.

Methods. NPG loaded with siRNAs targeted against FAK, NOTCH-1, and SOX-2 were prepared by the self-assembly of siRNAs with protamine–hyaluronic acid combination. Electron microscopy, DLS, and agarose gel electrophoresis were used for the physicochemical characterization. Cell transfection and gene-silencing efficiency were studied using human mesenchymal stem cells and rat C6 glioma-derived GSCs. Neurosphere inhibition was tested in vitro using GSCs derived from C6 cell line and glioma patient samples. Patient-derived xenograft model and orthotopic rat glioma model were used to test the effect of NPG on in vivo tumorigenicity.

Results. The siRNA nanoparticles with an average size ~ 250 nm and ~ 95% loading efficiency showed cellular uptake in ~95.5% GSCs. Simultaneous gene silencing of FAK, NOTCH-1, and SOX-2 led to the inhibition of neurosphere formation by GSCs, whereas normal stem cells remained unaffected and retained neuronal differentiation capability. GBM PDX models manifested significant impairment in the tumorigenic potential of NPG treated GSCs. Intracranial injection of NPG inhibited tumor growth in orthotopic rat brain tumor model.

Conclusion. Intracranially injectable n-siRNA NPG targeted to multiple stem-cell signaling impairs glioma initiation capabilities of GSCs and inhibited tumor growth in vivo.

Key Points

- siRNA nanoparticle gel (NPG) silenced NOTCH-1, SOX-2, and FAK genes in GSC.
- NPG inhibited tumorigenicity of GSCs in a PDX model.
- Intracranially injected NPG inhibited tumor growth in a rat orthotopic glioma model.

Glioblastoma (GBM) is one of the most aggressive types of brain tumor characterized by overall survival of 12–15 months and ~ 100% recurrence.[1] Among many hypotheses on the molecular and cellular basis of glioma recurrence, the contribution by tumor-initiating glioma stem-like cells (GSC) characterized by the expression of CD133+/-, NOTCH-1, SOX-2,

Importance of the Study

One of the primary causes of tumor recurrence in GBM is attributed to residual glioma stem cells. Nanoparticle siRNA-conjugate-based intracranial silencing of target genes is a promising approach to inhibit GSCs. Here, we demonstrate a multi-targeted siRNA nanoparticle gel (NPG) for the combinatorial intracranial silencing of aberrant genes in GSCs. NPG can be directly applied to the brain tumor resected cavity and the gel can diffuse through the brain tissue to inhibit the GSC population. Silencing of multiple genes simultaneously will avoid the escape of GSCs through compensatory mechanisms. The local application directly at the tumor area will reduce the possibility of off-target effects.

Nestin, and Musashi attracted significant attention.[2,3] This unique subset of cells possess substantial resistance toward chemo- and radiation therapy.[4] It is almost certain that GSCs evade current therapies leading to inevitable tumor recurrence.

Considering efficient chemo-drug efflux mechanisms in GSCs, a potential alternative approach is to silence key genes associated with stemness using siRNAs. Recently, nanoparticle-based siRNA therapeutics received US-FDA approval to treat hereditary amyloidosis,[5] indicating the translation potential of siRNA therapeutics. However, in GSCs, silencing of any single gene will not be sufficient to inhibit their growth; rather, multiple aberrant pathways related to the maintenance of stemness and survival need to be silenced almost simultaneously.[6] The feedback loop mechanisms trigger the hyper-activation of compensatory pathways, enabling GSCs to escape from particular gene-targeted RNAi. As a proof of concept, we have selected 3 critical target genes, NOTCH-1, SOX-2, and FAK for the nanoparticle-based combinatorial RNAi as they are reported to be aberrant in GSCs.[7–9] NOTCH-1, an evolutionarily conserved gene playing an essential role in neuronal stem cell self-renewal, was found to be highly over-expressed in GSCs and contribute to chemo-and radiation resistance.[10,11] SOX-2 is another important neural stem cell marker, playing a critical role in maintaining stemness in GSCs.[8,12] Focal adhesion kinase (FAK) is another important signaling involved in the neurogenesis and adhesion-mediated drug resistance (AMDR).[9,13] FAK-targeted therapeutics were proposed to eliminate cancer stem cells and some of the inhibitors are under clinical trials.[9] As these 3 genes are also inter-regulated, we hypothesize that silencing of any one alone may not be sufficient enough as the compensatory mechanisms may activate other downstream pathways to escape cell death. Therefore, silencing all the 3 stemness-associated genes makes more sense as the compensatory mechanisms causing hyperactivations can be blocked.

Systemic administration of multiple siRNA sequences to the brain is challenging due to the blood–brain barrier and potential off-target toxicity. Earlier, we have shown that multifunctional, injectable, or implantable nanosystems can be used for the localized release of therapeutics in liver and brain.[14,15] Taking those inputs, here, we report the development of an intracranially injectable nanoparticle gel (NPG) co-loaded with 3 different siRNAs against NOTCH-1, SOX-2, and FAK (n-siRNA$_{FNS}$) for the localized RNAi in the brain-tumor to target GSCs. Yu et al. reported a similar approach where they targeted a different set of genes using lipopolyplex nanoparticles, delivered by the convection-enhanced method.[16] Here, we followed a simple stereotactic injection of NPG directly into the brain tumor. Further, compared to the lipid-based nanosystems, we used an FDA-approved cationic peptide, protamine sulphate (PS), for the siRNA delivery.[17] Another biocompatible material, hyaluronic-acid, which is a key constituent of brain extra-cellular matrix, was used to form desired gel consistency suitable for intracranial injection. The translational potential of both these carrier nanomaterials was given primary importance while the novelty aspect was centered around the idea of simultaneous RNAi of NOTCH-1, SOX-2, and FAK in glioma-stem cells locally in the brain. Although these 3 critical pathways are aberrant in glioma stem cells, the same is also important for normal neural stem cells. Hence, the intra-brain dispersion of NPG had to be controlled to avoid off-target toxicity effects with an effective diffusion of ~2–3 cm from the surgical margin where residual GSCs reported to trigger recurrence.[18]

Methods

Preparation of n-siRNA and NPG

n-siRNA was prepared in nuclease-free aqueous solution using electrostatic interaction chemistry. Briefly, the cationic peptide in nuclease-free water was added in excess (5 mg/mL) dropwise under constant stirring into siRNA (20 μM) (siGenome SMART pool siRNA, Dharmacon) at N/P ratios of 10 or 20, at 4°C, 1 h. The nanoparticle formed was purified by centrifugation. For the n-siRNA NPG preparation, 5% hyaluronic acid in sterile nuclease-free water was prepared under stirring in RNase-free sterile environment; added dropwise under constant vortexing at 2500 rpm to form a gel. siRNA loading efficiency in n-siRNA was analyzed using agarose gel electrophoresis (Supplementary Material).

Cell Culture

Human mesenchymal stem cells were cultured as previously reported.[19] C6 cells obtained from the American Type Culture Collection were cultivated in DMEM-F12 medium supplemented

with 10% fetal bovine serum, glutamine, penicillin, and streptomycin at 37°C and 5% CO_2. Cells were passaged and cultured in neurosphere-forming media, and clonogenic potential was also assessed as described previously.[20]

Primary Glioma Cell Isolation and Culture

GBM patient samples were collected with prior consent from patients and approval from the institutional ethical committee of Amrita Institute of Medical Sciences, Kochi. Immediately after resection, tumors were collected in DMEM-F12 complete media and cultured as previously reported.[21]

Assessment of Cell Viability

C6 neurosphere inhibition and assessment of cell viability

In 24-well plate, 5000 cells were seeded and n-siRNA$_{scrambled}$ (375nM–equivalent to the combinatorial n-siRNA), n-siRNA$_{FAK}$, n-siRNA$_{NOTCH-1}$, n-siRNA$_{SOX-2}$, n-siRNA$_{FNS}$ (125 nM each) double treatment (DT) was given after 24 h of seeding. In the case of combination treatment initially, temozolomide was treated for 72 h, media removed and fresh media was added and treated with n-siRNA$_{FNS}$ (DT). Live/dead assay performed on day 14.

Patient sample-derived neurosphere inhibition assay.— In a 24-well plate (BD Falcon) 1×10^4 cells were seeded and respective treatments given as mentioned in C6 neurosphere inhibition protocol. Details are given in Supplementary Methods.

Confocal Imaging of Intracellular n-siRNA Delivery

Mesenchymal stem cells or C6 neurospheres were treated with n-siRNA-Cy5.5 (100 nM) and incubated for 4 h at standard culture conditions. The cells were imaged under confocal microscope (TCS SP5, Leica) at an excitation of 647 nm.

Wound Healing Assessment

C6 glioma cells or hMSCs studied for its migration post-n-siRNA$_{FAK}$.[22] n-siRNA$_{scrambled}$ was kept as control and n-siRNA$_{FAK}$ as treatment (100 nM-DT) after seeding and migration of cells were monitored over a period of 48 h.

Quantitative Real-time PCR

hMSCs or C6 cells were treated with n-siRNA$_{FAK/NOTCH-1/SOX-2}$ and siRNA$_{FNS}$ (100 nM-DT) and quantified using qRT-PCR as described in the Supplementary Material.

Flowcytometry Studies

The cells used for flowcytometry analysis were immunostained as previously reported[23] (Supplementary Method). For n-siRNA uptake studies, Alexa fluor-555-tagged siRNA was used for n-siRNA preparation. On day 7, the C6 neurospheres were treated with fluorescent-tagged n-siRNA. After 4 h of incubation, the neurospheres were trypsinized and single cells were washed and analyzed using flowcytometry.

Neurogenic Differentiation Assay

hMSCs (10,000 cells) were seeded in 12-well plate, and after 24 h, double transfected with n-siRNA$_{FNS}$ (125 nM each) and proceeded as detailed in the Supplementary Methods.

Immunostaining

Immunostaining was performed on cells grown on acid-etched coverslips (Supplementary Methods).

Injection and Diffusion of NPG in Brain Tissue

NPG was prepared with AF555-conjugated siRNA (BLOCK-iT AlexaFluor, Thermo Fischer Scientific). Rat brain was used to inject the NPG to study diffusion ex vivo, where, 7 µL NPG was injected (Supplementary Method).

In Vivo Studies

All the animal studies were conducted under the guidance of the Institutional Animal Ethics Committee of Amrita Institute of Medical Sciences and Research Centre, Kochi, India and the protocols followed were in accordance with the institutional guidelines and humane handling of animals were performed.

In vivo studies in PDX models were carried out in 4–6-week-old male Balb/c nu/nu mice. The animals were randomly divided into 5 groups (untreated, n-siRNA$_{scrambled}$, TMZ, n-siRNA$_{FNS,}$ TMZ+n-siRNA$_{FNS}$). The antitumoractivity assessments of n-siRNAs were carried out in the intracranial C6 glioma model. Detailed protocol of in vivo study is provided in the Supplementary Methods.

Statistical Analysis

Data were analyzed using Student *t*-test when comparing 2 groups and by ANOVA, when comparing more than 2 groups. Data are expressed as mean ± standard deviation or mean ± standard error of the mean. The differences were considered significant at $P < .05$.

Results

Synthesis and Characterization of siRNA Nanoparticles (n-siRNA) and NPG

Figure 1A shows the schematic diagram of nanoparticle formation depicting a simple process involving the self-assembly of multiple siRNA sequences (FAK, NOTCH-1, and

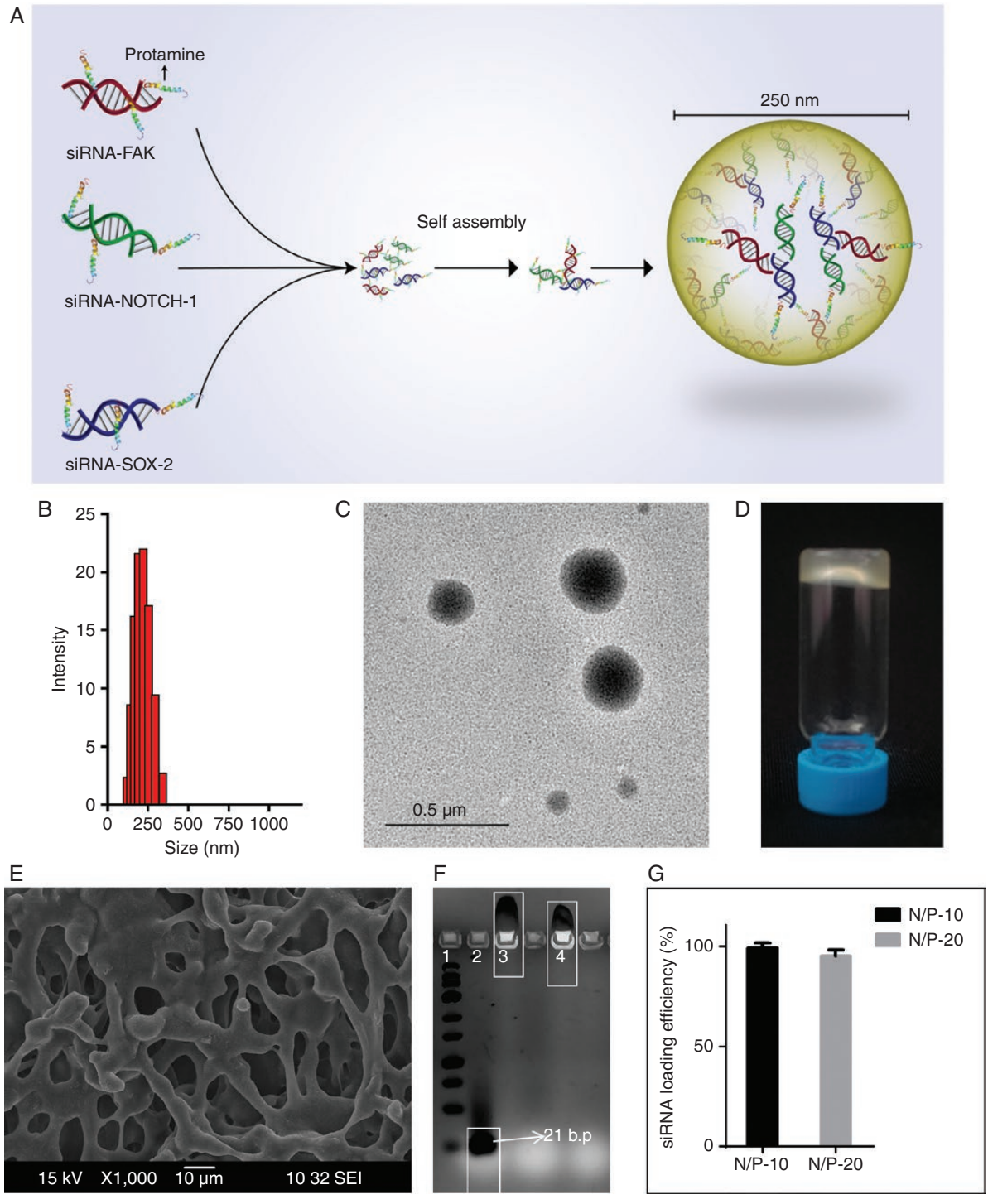

Figure 1. Physicochemical characterization of n-siRNA. (A) Schematic representation of n-siRNA formed by the self-assembly of siRNA against FAK, NOTCH-1, and SOX-2. (B) DLS showing the size distribution of nanoparticle (average 250nm) at N/P ratio 20. (C) Representative TEM image of n-siRNA. (D) Intracranially injectable n-siRNA-loaded nanoparticle gel (NPG) prepared using hyaluronic acid. (E) SEM image of lyophilized NPG showing macroporous structure. (F) Agarose gel electrophoresis showing complexation of siRNA: lane 1–RNA ladder, lane 2-naked siRNA, lane 3-n-siRNA (N/P-10), lane 4-n-siRNA (N/P-20). (G) siRNA loading efficiency in nanoparticle prepared at N/P:10 and 20. Data are mean ± standard deviation.

SOX-2) with protamine sulfate under physiological pH. The nanoparticles showed an average size of ~250 nm (Figure 1B and C). Electron dispersion spectroscopy revealed (Supplementary Figure S1) the co-existence of carbon, nitrogen, oxygen, phosphorus, and sulfur, where phosphorous reflected the RNA content, and sulfur indicated protamine sulfate. Figure 1D shows hyaluronic acid-based NPG with ~ 98wt% loading of n-siRNA nanoparticles.

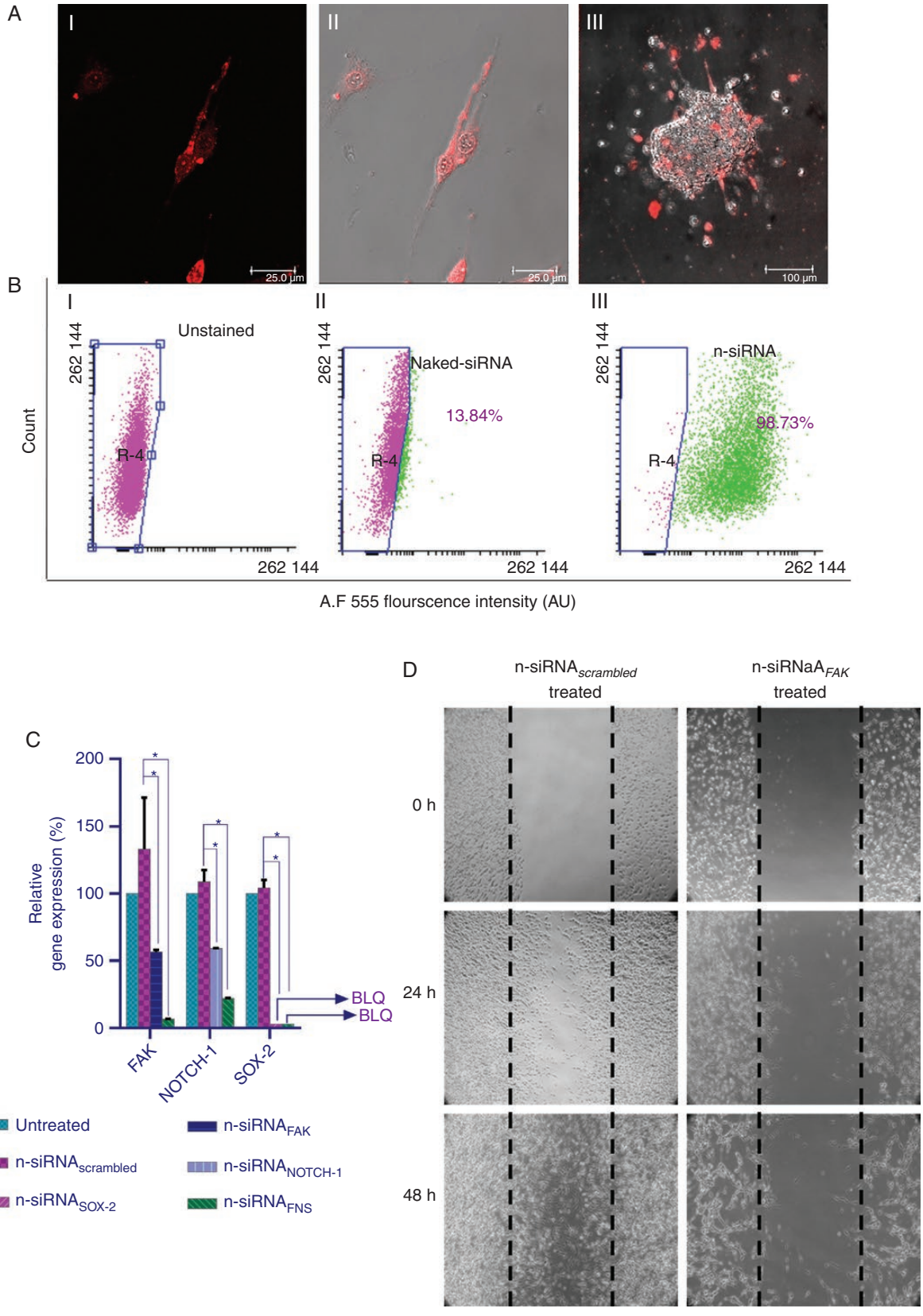

Figure 2. n-siRNA uptake and functional activity in rat C6 glioma cells. (A) Representative confocal images showing n-Cy5-siRNA uptake in (i) C6 cells (red) (ii) corresponding merged image (iii) merged confocal image in C6 neurospheres. (B) Flow analysis of n-siRNA uptake showing

Lyophilized NPG exhibited a porous structure (Figure 1E), which was transformed into an injectable consistency upon infusion with sterile water. In gel electrophoresis (Figure 1F), n-siRNA prepared at N/P ratio = 10 (lane-3) or 20 (lane-4) manifested strong electrostatic complexation compared to naked siRNA (lane-2). siRNA loading efficiency in the nanoparticle was ~ 95% for both N/P = 10 or 20 (Figure 1G) and zeta potential was 28 ± 4.5 mV for N/P = 20 and 25 ± 6.5 mV for N/P = 10. n-siRNA prepared with N/P = 20 having ~7.7wt% siRNA was used for all further experiments.

n-siRNA-mediated RNAi in Stem Cells

Initial studies on nanoparticle-mediated RNAi were done on 2 model cells: (i) rat glioma cell line C6 with high nestin positivity and (ii) human mesenchymal stem cells (hMSC). It is an axiom that primary stem cells are one of the most difficult-to-transfect cells.[24] Hence, we used hMSCs to test the intracellular uptake, functional RNAi, and potential toxicity effects. Glioma cell line, C6 with high expression of stem cell markers was used to test whether simultaneous gene silencing of stem cell signaling will inhibit tumorigenesis of C6.[20] C6 was reported to have > 90% cells expressing stem cell markers such as nestin[25,26] and ability to form neurospheres from single cells, which we also confirmed in our neurosphere cultures with C6 (Supplementary Figure S2A-C). These features make C6 cell line a representative GSC-like model for the initial testing of n-siRNA.

One of the challenges in siRNA therapeutics is the low transfection efficiency, particularly in case of stem cells.[24] However, *n*-siRNA (100 nM) treated hMSCs displayed excellent uptake (~ 91.7%) (Supplementary Figure S3A) and successful gene silencing with down-regulation of all the 3 target genes; FAK (97%), NOTCH-1 (56%), or SOX-2 (99.7%) (Supplementary Figure S3B) observed. In cell migration assay, *n*-siRNA$_{FAK}$ treated cells were unable to migrate into the wound space unlike the case of *n*-siRNA$_{scrambled}$ (Supplementary Figure S3C). The toxicity effect of RNAi at various concentrations in hMSC (Supplementary Figure S3D) showed that, although down-regulation of gene expression observed at 100 nM, the cytotoxicity (40%) was observed at 250 nM. As the treatment plan was directed toward brain tumor, we tested the effect of *n*-siRNA$_{FNS}$ on the ability of hMSCs to differentiate into neurons (Supplementary Figure S3E). Interestingly, the treated hMSCs retained their potential to differentiate into neurons as good as that of untreated cells.

Intracellular uptake of Cy5.5-tagged *n*-siRNA in rat C6 and 3D neurospheres showed excellent uptake in > 90% cells (Figure 2A, i–iii). Z-stack image of all the planes of the spheroid together showed better information about the cellular uptake along with fluorescence intensity of Cy5.5 (Supplementary Video 1, Supplementary Figure S4). Further, flow cytometry analysis confirmed the uptake of *n*-siRNA in 98.7% of cells, whereas only 13.8% naked siRNA uptake was observed within 4 h (Figure 2B). Gene expression studies revealed 55% and 58% of FAK and NOTCH-1 levels in cells transfected with respective n-siRNA$_{FAK}$ or n-siRNA$_{NOTCH-1}$, whereas n-siRNA$_{SOX-2}$-treated cells exhibited below the detectable level of SOX-2 (Figure 2C). The combinatorial silencing of FAK, NOTCH-1, and SOX-2 using n-siRNA$_{FNS}$ resulted in the down-regulation of gene expression levels of FAK-94%, NOTCH-1–88%, SOX-2–BLQ. This clearly shows the successful combinatorial RNAi in selected gene targets. Wound healing studies on *n*-siRNA$_{FAK}$-treated C6 cells (Figure 4D) manifested a significant effect on the migratory and adherent properties of cells compared to *n*-siRNA$_{scrambled}$.

Effect of *n*-siRNA-based Gene Silencing in Rat Glioma Neurospheres

The effect of singular and combinatorial n-siRNA treatment on neurospheres formation was studied first in rat C6 cells. We also examined whether the current clinical drug, Temozolomide (TMZ), has any contributory effect with n-siRNA$_{FNS}$ in neurosphere inhibition. Figure 3A shows neurospheres treated with singular n-siRNA, n-siRNA$_{FNS,}$ TMZ alone, or TMZ in combination with n-siRNA$_{FNS.}$ Untreated (Figure 3A, i) and n-siRNA$_{scrambled}$ (Figure 3A, ii) treated cells displayed the natural progression of neurosphere within 4–8 days, whereas TMZ treated cells exhibited relatively slow growth in the initial days though conspicuously regained proliferation by day 8 (Figure 3A, iii). Singular n-siRNA treatment, though slowed neurosphere formation compared to the control, by day 14 the neurospheres were vivid (Figure 3A, iv–vi). In contrast, n-siRNA$_{FNS}$ (Figure 3A, vii), as well as TMZ+n-siRNA$_{FNS}$ (Figure 3A, viii) treated neurospheres registered inhibition of neurosphere formation. Relative neurosphere size per unit area, normalized to the untreated control, on day 14 (Figure 3B) was ~ 20% less in the case of TMZ-treated group, whereas > 90% was found in n-siRNA$_{FNS}$ or TMZ+n-siRNA$_{FNS}$ groups. MTT assay (Figure 3C) performed on day 4, 8, and 14 has reflected the observed effects on the neurospheres. Significant cell death was noted in n-siRNA$_{FNS}$ as well as TMZ+n-siRNA$_{FNS}$ combination. A similar observation was found in live/dead assay performed on day 14 of the treatment (Supplementary Figure S5A).

Testing of *n*-siRNA in GBM Patient-derived Neurospheres

Four GBM patient-derived neurospheres (PDN) were used for testing the efficacy of n-siRNA combination. PDNs were characterized by the stem and progenitor markers; CD133, Nestin, SOX-2, NOTCH-1, and GFAP (Supplementary Figure S5B and C). Though the expression levels varied,

(i) unstained, (ii) naked-siRNA, and (iii) n-siRNA (Alexaflour 555) in C6 neurospheres, indicating uptake in 98.7% cells. (C) Relative gene expression levels of FAK, NOTCH-1, and SOX-2 gene analyzed by quantitative real-time PCR after treatment with n-siRNA$_{FAK}$, n-siRNA$_{NOTCH-1}$ or siRNA$_{SOX-2}$ (100 nM each), *P < .05 compared to corresponding untreated. (D) Wound healing assay showing inhibition of cell migration in n-siRNA$_{FAK}$ treated C6 glioma cells. Data are mean ± standard deviation.

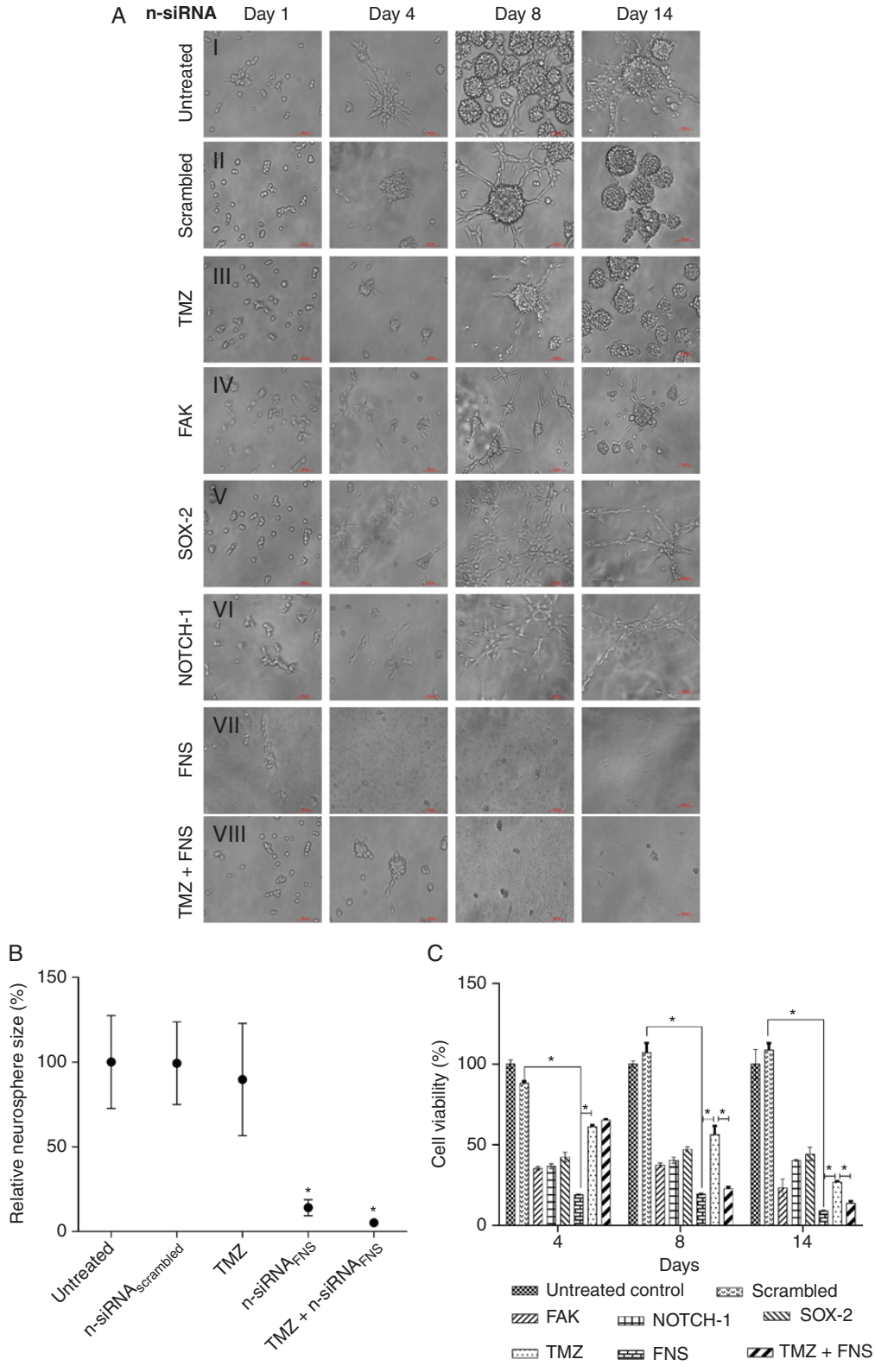

Figure 3. Neurosphere inhibition assay in C6 glioma cell line. (A) Neurosphere imaged at different time intervals Day (1–14): (i) untreated (ii) n-siRNA$_{scrambled}$ (iii) TMZ (iv) n-siRNA$_{FAK}$ (v) n-siRNA$_{NOTCH-1}$ (vi) n-siRNA$_{SOX-2}$ (vii) n-siRNA$_{FAK+NOTCH-1+SOX-2}$ (FNS) (viii) TMZ treated for 72 h followed by n-siRNA$_{FNS}$. (B) Relative percentage spheroid area on day-14 post-treatment, where area of untreated spheres was considered as 100% (data are mean ± SEM) (C) C6 neurosphere viability on day-4, 8, and 14 post-treatment with individual n-siRNA or the final combination of n-siRNA$_{FNS}$ without TMZ. *$P < .05$, data are mean ± standard deviation.

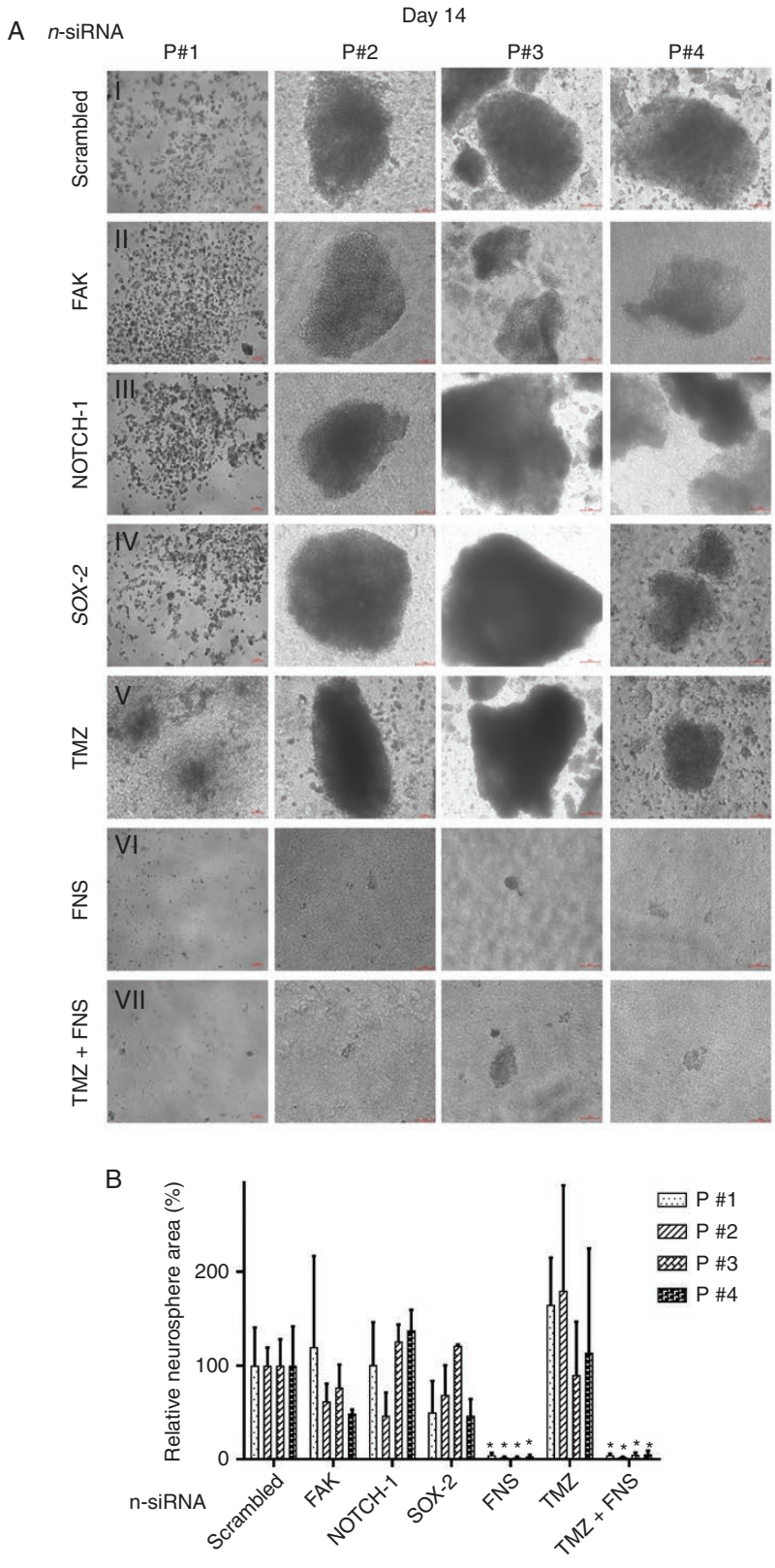

Figure 4. Inhibition of neurospheres in patient-derived glioma stem-like cells. (A) Representative micrographs of neurosphere formation on day-14 post (i) n-siRNA$_{scrambled}$ (ii) n-siRNA$_{FAK}$ (iii) n-siRNA$_{NOTCH-1}$ (iv) n-siRNA$_{SOX-2}$ (v) TMZ (vi) n-siRNA$_{FNS,}$ and (vii) TMZ+n-siRNA$_{FNS}$. (B) Corresponding graphical representation of relative percentage neurosphere area, where the area of n-siRNA$_{scrambled}$-treated group is assigned as 100%. Data are mean of 3 sample per patient ± standard deviation, $^{*}P < .001$ against n-siRNA$_{scrambled}$.

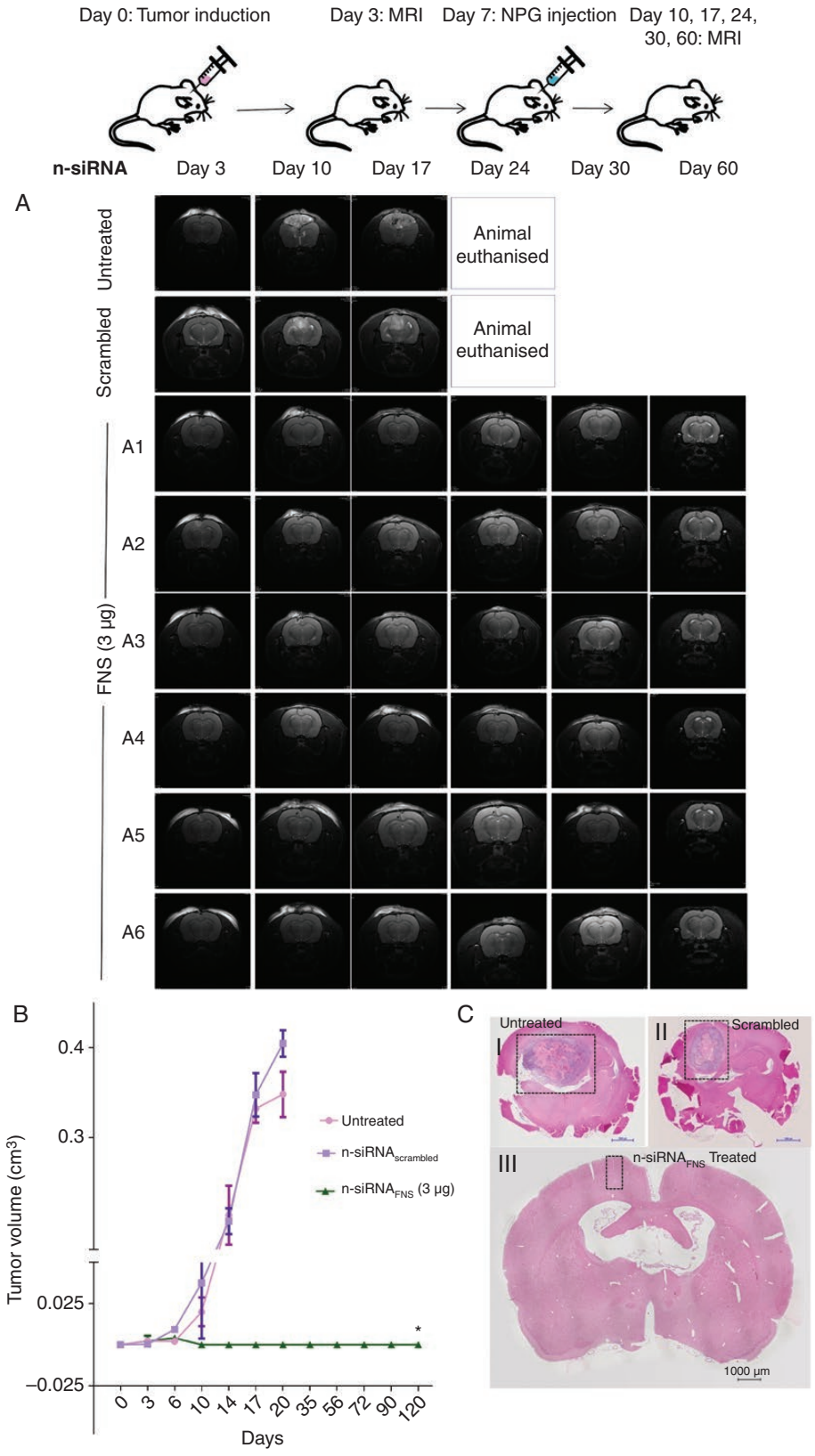

Figure 5. In vivo antitumour effect of intracranial n-siRNA treatment: (A) Representative T2 weighted MR images of Day 3–60 for the untreated, n-siRNA$_{scrambled}$ and n-siRNA$_{FNS}$ based NPG (3µg) injected into orthotopic rat glioma (C6). Tumour growth can be seen in untreated and n-siRNA$_{scrambled}$ groups by Day-10 leading to mortality around Day-20, in contrast, n-siRNA$_{FNS}$ treated group (A1-A6) showed no significant tumour

all the samples showed the presence of GSCs expressing the above markers in PDNs. The size and progression of PDNs varied from patient to patient as larger neurosphere was formed in P#2, P#3 and P#4 whereas P#1 showed only micro-aggregates of cells even upto day 14. This is attributed to the heterogenicity of patient samples. However, all patient models showed the characteristic GBM markers along with the in vivo tumor-forming abilities. Treatment of PDNs with n-siRNA$_{scrambled}$, n-siRNA$_{FAK}$, n-siRNA$_{NOTCH-1}$, or n-siRNA$_{SOX-2}$ did not show any significant effect till day 8 (Supplementary Figures S6 and S7). Interestingly, current clinical drug TMZ had little effect on PDN progression, whereas n-siRNA$_{FNS}$ and TMZ. + n-siRNA$_{FNS}$-treated groups exhibited a significant reduction of PDN size in all 4 cases. Day 14 data, shown in Figure 4A, suggest that n-siRNA$_{scrambled}$ or singular n-siRNAs had no therapeutic effect on all 4 PDNs. TMZ alone also had fairly conspicuous neurosphere formation compared to *n*-siRNA$_{scrambled}$ on day 14. At the same time, n-siRNA$_{FNS}$ (Figure 4A, vi) or TMZ+n-siRNA$_{FNS}$ (Figure 4A, vii) groups were unable to sustain the PDN compared to the respective n-siRNA$_{scrambled}$ control. Further, the relative neurosphere area in each patient sample on day 14 was calculated (Figure 4B). Compared to the untreated neurosphere area (100%), n-siRNA$_{FNS}$ showed only < 2% neurosphere area in all 4 patient samples.

In Vivo Studies on *n*-siRNA-based RNAi in Patient-derived Xenograft Models

We conducted 2 types of in vivo experiments to study: (i) the effect of n-siRNA treatment on human GSC's ability to form xenograft tumor in nude mice and (ii) the effect of n-siRNA treatment on the growth of an established orthotopic glioma in rat model. For the first case, we cultured patient-derived neurospheres (Supplementary Figure S9A) in a preoptimized 3D scaffold ex vivo (Supplementary Figure S8A and B), which provided a brain-ECM mimicking niche for the tumor growth (Supplementary Figure S8C and D). Compared to direct injection of patient-derived single cells or Matrigel supported implantation, the 3D scaffold provided 100% success rate in the formation of PDX in nude mice without the use of severe combined immune-deficient mice (SCID). After 7 days of culture, the 3D tumor was transplanted subcutaneously in mice with or without the n-siRNA treatment and studied if the treatment impaired the ability of GSCs to establish xenograft tumor in vivo (Supplementary Figure S9B). The PDX tumors formed by this method showed typical GBM pathology of patients (Supplementary Figure S9C). The cells isolated from these xenografts also displayed the capacity to form secondary neurospheres ex vivo (Supplementary Figure S9D). Also, the PDX tumor-derived cells showed expression of GSC markers (CD133$^+$ and Nestin$^+$) (Supplementary Figure S9E) similar to that of primary GBM cells (Supplementary Figure S5B). Untreated or treated 3D cultures were implanted in Balb/c nu/nu mice and examined the tumor growth till day 30 as depicted in Figure 5F. Representative images of animals on day 30 from each group are shown in Supplementary Figure S9G and tumor growth is plotted in Supplementary Figure S9H. Untreated and *n*-siRNA$_{scrambled}$-treated samples recorded tumor size of ~ 2.5 cm^3 in vivo by day 30. TMZ treated culture had a marginal reduction in tumor size (~1.5 cm^3), whereas *n*-siRNA$_{FNS}$ or TMZ+*n*-siRNA$_{FNS}$ treated 3D cultures exhibited no tumor growth in mice (Supplementary Figure S9H). As the 3D tumor was implanted in the animal with the support of a scaffold, the site of implantation showed some minor projection in all PDXs; however, the same was not due to the residual tumor but that of the scaffold as confirmed by postmortem examination. In effect, we show that the pretreatment with n-siRNA$_{FNS}$ critically impaired the ability of GSC to form PDX tumor in xenograft model.

Diffusion of n-siRNA gel (NPG) in Brain Tissue Phantom

Before testing the n-siRNA in orthotopic glioma model, we studied the controlled diffusion of nanoparticles in brain tissue. Alexaflour 555-conjugated siRNA-NPG was injected ex vivo in a rat brain phantom (Supplementary Figure S10A). Fluorescence from NPG-AF555 was detected under a stereo-fluorescent microscope after 2 h (Supplementary Figure S10B–D), where the NPG showed a diffusion of ~3.02 mm × ~1.46 mm. Supplementary Figure S10E shows a fluorescent microscopic image of NPG AF555 diffusion in brain phantom, wherein distribution into the tissue was observed. The results suggest that locally injected NPG could diffuse into the tissue region in a controlled manner. However, this could also be attributed to any depreciation in viability of tissue over 2 h, allowing passive spread of the injected material. However, in histopathology analysis of brain tissue, no observable changes in the tissue structure or integrity was observed in the tested incubation conditions.

Intracranial Injection of *n*-siRNA Gel and Tumor Inhibition in Rat Orthotopic Tumor Model

In order to test the feasibility of direct intracranial injection of siRNA nano-gel and its efficacy in orthotopic glioma model, we have stereotactically implanted C6 glioma neurospheres in rat brain and the tumor growth was visible by day 6 in 7T animal MRI (Supplementary Figure S11A). As we have observed better efficacy of combinatorial n-siRNA$_{FNS}$ compared to single-gene-targeted siRNA in both C6 neurosphere, as well as PDN models, the rat intracranial study was limited to the final formulation of n-siRNA$_{FNS}$. The NPG containing either 50 ng siRNA was administered on the same day or 3 µg siRNA injected on day 7 post-tumor induction when tumor size of

growth till 120 days (B) Graph showing quantitative tumour volume in orthotopic glioma in different treatment groups, estimated from MRI (C) H&E of brain sections showing tumour growth in (i) untreated (ii) n-siRNA$_{scrambled}$ (iii) n-siRNA$_{FNS}$ groups.*P < .001, data are mean ± SEM.

~ 1.9 mm^3 was confirmed by MRI (Supplementary Figure S11A). MRI shows that neither n-siRNA$_{FNS}$-NPG (50 ng) (Supplementary Figure S12A and B) nor n-siRNA$_{FNS}$ –NPG (3 μg)-treated group manifested any tumor growth in any of the treated animals (Figure 5A), whereas by day 17, the untreated and n-siRNA$_{scrambled}$ NPG had significant tumor growth measuring ~ 0.5 cm^3 and ~0.4 $cm,^3$ respectively. The tumor volume graph (Figure 5B), showed a similar pattern of tumor growth in untreated and n-siRNA$_{scrambled}$ NPG and null growth in n-siRNA$_{FNS}$ until day 120. The histopathological analysis also revealed significant tumor size in control (Figure 5C, i–ii), whereas the treated group exhibited no trace of tumor (Figure 5C, iii). Clearly, the study shows that intracranial injection of n-siRNA$_{FNS}$-NPG could inhibit established brain tumor in rat, though the day 0 treatment of n-siRNA only reflects the efficient cellular uptake and death owing to RNAi than antitumor efficacy.

Discussion

High-grade brain tumor-associated mortality majorly occurs due to tumor recurrence, contributed by residual GSCs, which escapes current treatment regimens. Here, we explored the possibility of simultaneous multi-gene silencing of stemness-associated genes in GSCs using intracranial injectable siRNA NPG. GSC targeted combinatorial siRNA nanoparticles were formed by the self-assembly of a clinically used cationic peptide, protamine sulfate, with 3 different siRNAs targeted to FAK, NOTCH-1, and SOX-2, which were known to be critical for maintaining stemness. To overcome the transfection efficiency-associated challenges, nanoparticles of average size, 250 nm and net cationic charge, 28 ± 4.5 mV, were prepared by adjusting the amino-to-phosphate ratio. These nanoparticles showed ~ 95% loading efficiency for siRNA.

Human mesenchymal stem cells were used as a model system to optimize the transfection efficiency since nonviral transfection efficiency was reported to be low in stem cells.[27,28] However, our n-siRNA system registered ~ 92% transfection efficiency and down-regulation of targeted gene expression (FAK, NOTCH-1, SOX-2) at the optimized nano-size and zeta potential. No significant toxicity was observed up to 125 nM n-siRNA$_{FNS}$ (DT), in normal stem cells, at which their neuronal differentiation capacity remained unaffected. Therefore, this concentration was used for all further studies in glioma stem cells and PDNs. Further testing on Nestin^{high} rat glioma stem-like cells and neurospheres also displayed excellent (98.7%) n-siRNA uptake. Singular n-siRNA treatment caused significant down-regulation of respective target genes (FAK/NOTCH-1 or SOX-2), indicating successful RNAi. Further, cell migration studies on n-siRNA$_{FAK}$ treated C6 cells and hMSCs exhibited a significant effect on the migratory and adherent properties of cells compared to n-siRNA$_{scrambled}$, clearly showing the physical manifestation of n-siRNA mediated RNAi in stem cells. Interestingly, an additional level of down-regulation was observed in FAK and NOTCH-1 in case of n-siRNA$_{FNS}$ combinatorial treatment, pointing toward an additive inhibitory effect. The level of SOX-2 remained at below the level of quantification (BLQ) for both singular and combinatorial treatments. The study reported by Tian et al. have provided insight into the cross-talk between FAK and NOTCH-1, where FAK was instrumental in the translocation of Notch Intracellular Domain (NICD-1) into the nucleus.[29] FAK also was reported to have an integral role in regulating NOTCH-1 expression. Studies in breast cancer cells show that silencing of NOTCH-1 resulted in inhibition of FAK activity.[30] NOTCH-SOX-2 pathway is observed to induce stemness and tumorigenicity in GBM,[31] whereas positive feedback loop mechanism between NOTCH-1 and SOX-2 in GSCs have also been reported.[32] It was observed that NOTCH-1 activate SOX-2 through SOX-9 and in turn, SOX-2 regulate NOTCH-1 expression through TET3-mediated DNA demethylation.[32] The additional down-regulation of FAK upon combinatorial silencing can also be associated with SOX-2 silencing, as FAK inhibition upon SOX-2 silencing has been reported.[33] All these surmises to the cross-talk between these pathways and thus justify our rationale of simultaneous multi-gene silencing using nanoparticles.[34]

The superiority of n-siRNA$_{FNS}$ over the singular treatments was reflected in C6 neurospheres and PDNs. Simultaneous gene silencing using n-siRNA$_{FNS}$ severely impaired the neurosphere formation and ~90% cells were coerced to undergo death. Generally, when a cell loses contact or adherence from the extracellular matrix, they undergo cell death, known as anoikis.[35,36] Anoikis resistance in cancer stem cells (CSCs) was reported, where the integrin repertoire is re-arranged and various molecular pathways are activated to survive.[7,37] Constitutive expression of NOTCH-1 in inhibiting anoikis was reported.[35,36] However, we believe that the simultaneous silencing of FAK, NOTCH-1, and SOX-2 could overcome anoikis resistance in stem cell neurospheres, leading to >90% cell death compared to individual silencing of NOTCH-1, FAK, or SOX-2.

TMZ resistance in glioma stem cells has been reported as one of the major causes for recurrence.[38] In our study, TMZ- treated C6 neurospheres and PDNs had an initial slow formation of neurosphere which later became vivid by day 8 and later flourished by day 14, which was reflected in the viability as well. The GSCs could be TMZ resistant and therefore TMZ did not significantly reduce neurosphere formation. This suggests that n-siRNA affected the clonogenic potential of human GSCs by the combinatorial silencing of FAK, NOTCH-1, and SOX-2. On the contrary, treatment with TMZ or single gene-targeted n-siRNAs had little effect compared to n-siRNA$_{FNS}$. More importantly, there was no tumor growth when n-siRNA$_{FNS}$ or TMZ+n-siRNA$_{FNS}$ pretreated PDNs (n = 3) were implanted subcutaneously in nude mice, showing an obvious difference compared to controls where tumor growth was registered in all 3 patient cases, showing inability of treated primary GSCs to form PDX tumor in vivo. To further affirm the same, the study has to be conducted in more number of PDXs to obtain statistically significant data. However, the study is not directly relevant to tumor inhibition in human glioma, though gives some light on the capability of n-siRNA performing RNAi in a 3 dimensional tumor-like environment. Further, for the localized intra-cranial/tumoral application, n-siRNA was formulated using hyaluronic acid. Localized delivery of n-siRNA NPG performed in brain phantom exhibited appreciable penetration up to ~3.02 mm ×1.46 mm within 2 h post-injection. In orthotopic rat C6

glioma model, administration of n-siRNA$_{FNS}$ NPG inhibited tumor growth when treated on an established tumor in brain on day 7, post-induction. This clearly indicates that effective gene-silencing happening in vivo with a single-dose injection of n-siRNA$_{FNS}$-NPG. Though intracranial gene silencing has been reported by Yu et al., to achieve significant tumor inhibition, convection-enhanced delivery using implanted osmotic pumps with continuous dosing of siRNA up to 70 µg/mouse over 14 days was needed. However, in the current approach, a low single dose—3 µg/rat of n-siRNA-NPG was effective in inhibiting the tumor formation. Further studies in patient derived orthotopic xenografts will be performed to further validate these data. Collectively, our study clearly shows the promise of locally injectable n-siRNA$_{FNS}$-NPG to provide effective combinatorial silencing of target genes, in glioma stem cells, leading to the inhibition of glioma neurosphere formation and tumor growth. In the clinical scenario, NPG can be introduced as localized adjuvant therapy post-tumour resection. This will be effective in targeting residual glioma stem cells at the surgical margin.

Supplementary Material

Supplementary material is available at *Neuro-Oncology Advances* online.

Keywords

cancer stem cells | gene silencing | nanoparticle | neurosphere | self-assembly

Acknowledgment

The authors acknowledge Mr. Sarath S, Ms. Arya Raju, Mr. Arun Lal, and Mr. K Sugavanan for their technical support.

Funding

The work presented in this manuscript was funded by the Department of Biotechnology, Govt of India under the project "Targeted Silencing of Cancer Stem Cell Signalling Using Novel Nano-siRNA conjugates" (BT/PR/2413/A.G.R./36/699/2011). MCA acknowledges University Grants commission for Senior Research fellowship (19-06/2011(i) EU-IV). The authors declare that there is no conflict of interest.

Authorship Statement. Concept, experimental design, writing manuscript: C.A.M. and M.K.; Clinical guidance: A.P. and K.P. Manuscript review: S.V.N. and K.K. MR imaging: G.S.G; Execution of experiments: C.A.M, K.J., R.R., A.M.A, M.M, and K.M.S.

References

1. Cohen MH, Johnson JR, Pazdur R. Food and Drug Administration Drug approval summary: temozolomide plus radiation therapy for the treatment of newly diagnosed glioblastoma multiforme. *Clin Cancer Res.* 2005;11(19 Pt 1):6767–6771.
2. Bao S, Wu Q, Sathornsumetee S, et al. Stem cell-like glioma cells promote tumor angiogenesis through vascular endothelial growth factor. *Cancer Res.* 2006;66(16):7843–7848.
3. Singh SK, Hawkins C, Clarke ID, et al. Identification of human brain tumour initiating cells. *Nature.* 2004;432(7015):396–401.
4. Chen J, Li Y, Yu TS, et al. A restricted cell population propagates glioblastoma growth after chemotherapy. *Nature.* 2012;488(7412):522–526.
5. Titze-de-Almeida SS, de Brandão PRP, Faber I, Titze-de-Almeida R. Leading RNA interference therapeutics part 1: silencing hereditary transthyretin amyloidosis, with a focus on patisiran. *Mol Diagnosis Ther.* 2020;24(1):49–59. doi: 10.1007/s40291-019-00434-w.
6. Trusolino L, Bertotti A. Compensatory pathways in oncogenic kinase signaling and resistance to targeted therapies: six degrees of separation. *Cancer Discov.* 2012;2(10):876–880.
7. Bouchard V, Demers MJ, Thibodeau S, et al. Fak/Src signaling in human intestinal epithelial cell survival and anoikis: differentiation state-specific uncoupling with the PI3-K/Akt-1 and MEK/Erk pathways. *J Cell Physiol.* 2007;212(3):717–728.
8. Berezovsky AD, Poisson LM, Cherba D, et al. Sox2 promotes malignancy in glioblastoma by regulating plasticity and astrocytic differentiation. *Neoplasia.* 2014;16(3):193–206, 206.e19.
9. Shibue T, Weinberg RA. EMT, CSCs, and drug resistance: the mechanistic link and clinical implications. *Nat Rev Clin Oncol.* 2017;14(10):611–629.
10. Bao ZZ, Cepko CL. The expression and function of Notch pathway genes in the developing rat eye. *J Neurosci.* 1997;17(4):1425–1434.
11. Fan X, Khaki L, Zhu TS, et al. NOTCH pathway blockade depletes CD133-positive glioblastoma cells and inhibits growth of tumor neurospheres and xenografts. *Stem Cells.* 2010;28(1):5–16.
12. Niu W, Zang T, Zou Y, et al. In vivo reprogramming of astrocytes to neuroblasts in the adult brain. *Nat Cell Biol.* 2013;15(10):1164–1175.
13. Golubovskaya VM. Targeting FAK in human cancer: from finding to first clinical trials. *Front Biosci (landmark ed).* 2014;19:687–706.
14. Ramachandran R, Junnuthula VR, Gowd GS, et al. Theranostic 3-Dimensional nano brain-implant for prolonged and localized treatment of recurrent glioma. *Sci Rep.* 2017;7:43271.
15. Ashokan A, Somasundaram VH, Gowd GS, et al. Biomineral nano-theranostic agent for magnetic resonance image guided, augmented radiofrequency ablation of liver tumor. *Sci Rep.* 2017;7(1):14481.
16. Yu D, Khan OF, Suvà ML, et al. Multiplexed RNAi therapy against brain tumor-initiating cells via lipopolymeric nanoparticle infusion delays glioblastoma progression. *Proc Natl Acad Sci Usa.* 2017;114(30):E6147–E6156.
17. Hagedorn HC, Jensen BN, Krarup NB, Wodstrup I. Protamine insulinate. *Acta Med Scand.* 1936;90(78S):678–684.
18. Brandes AA, Tosoni A, Franceschi E, et al. Recurrence pattern after temozolomide concomitant with and adjuvant to radiotherapy in newly diagnosed patients with glioblastoma: correlation With MGMT promoter methylation status. *J Clin Oncol.* 2009;27(8):1275–1279.
19. Binulal NS, Natarajan A, Menon D, Bhaskaran VK, Mony U, Nair SV. PCL-gelatin composite nanofibers electrospun using diluted acetic acid-ethyl acetate solvent system for stem cell-based bone tissue engineering. *J Biomater Sci Polym Ed.* 2014;25(4):325–340.

20. Zheng X, Shen G, Yang X, Liu W. Most C6 cells are cancer stem cells: evidence from clonal and population analyses. *Cancer Res.* 2007;67(8):3691–3697.
21. Galli R, Binda E, Orfanelli U, et al. Isolation and characterization of tumorigenic, stem-like neural precursors from human glioblastoma. *Cancer Res.* 2004;64(19):7011–7021.
22. Malarvizhi GL, Chandran P, Retnakumari AP, et al. A rationally designed photo-chemo core-shell nanomedicine for inhibiting the migration of metastatic breast cancer cells followed by photodynamic killing. *Nanomedicine.* 2014;10(3):579–587.
23. Chandran P, Gupta N, Retnakumari AP, et al. Simultaneous inhibition of aberrant cancer kinome using rationally designed polymer-protein core-shell nanomedicine. *Nanomedicine.* 2013;9(8):1317–1327.
24. Yoshikawa T, Uchimura E, Kishi M, Funeriu DP, Miyake M, Miyake J. Transfection microarray of human mesenchymal stem cells and on-chip siRNA gene knockdown. *J Control Release.* 2004;96(2):227–232.
25. Kondo T, Setoguchi T, Taga T. Persistence of a small subpopulation of cancer stem-like cells in the C6 glioma cell line. *Proc Natl Acad Sci Usa.* 2004;101(3):781–786.
26. Neradil J, Veselska R. Nestin as a marker of cancer stem cells. *Cancer Sci.* 2015;106(7):803–811.
27. Hamann A, Nguyen A, Pannier AK. Nucleic acid delivery to mesenchymal stem cells: a review of nonviral methods and applications. *J Biol Eng.* 2019;13:7.
28. Walker K, Hjelmeland A. Method for efficient transduction of cancer stem cells. *J Cancer Stem Cell Res.* 2014;2. doi: 10.14343/JCSCR.2014.2e1008.
29. Tian Y, Wang W, Lu Q, et al. Cross-talk of SFRP4, integrin $\alpha 1\beta 1$, and Notch1 inhibits cardiac differentiation of P19CL6 cells. *Cell Signal.* 2016;28(11):1806–1815.
30. Wang J, Fu L, Gu F, Ma Y. Notch1 is involved in migration and invasion of human breast cancer cells. *Oncol Rep.* 2011;26(5):1295–1303.
31. Bazzoni R, Bentivegna A. Role of notch signaling pathway in glioblastoma pathogenesis. *Cancers (Basel).* 2019;11(3):292. doi: 10.3390/cancers11030292.
32. Wang J, Xu SL, Duan JJ, et al. Invasion of white matter tracts by glioma stem cells is regulated by a NOTCH1-SOX2 positive-feedback loop. *Nat Neurosci.* 2019;22(1):91–105.
33. Oppel F, Müller N, Schackert G, et al. SOX2-RNAi attenuates S-phase entry and induces RhoA-dependent switch to protease-independent amoeboid migration in human glioma cells. *Mol Cancer.* 2011;10:137.
34. Sathornsumetee S, Reardon DA. Targeting multiple kinases in glioblastoma multiforme. *Expert opin Investig Drugs.* 2009;18(3):277–292.
35. Frisch SM, Francis H. Disruption of epithelial cell-matrix interactions induces apoptosis. *J Cell Biol.* 1994;124(4):619–626.
36. Paoli P, Giannoni E, Chiarugi P. Anoikis molecular pathways and its role in cancer progression. *Biochim Biophys Acta.* 2013;1833(12):3481–3498.
37. Herrera VL, Decano JL, Tan GA, et al. DEspR roles in tumor vasculo-angiogenesis, invasiveness, CSC-survival and anoikis resistance: a 'common receptor coordinator' paradigm. *PLoS One.* 2014;9(1):e85821.
38. Yamada R, Nakano I. Glioma stem cells: their role in chemoresistance. *World Neurosurg.* 2012;77(2):237–240. doi: 10.1016/j.wneu.2012.01.004.